



ELSEVIER

Contents lists available at ScienceDirect

Measurement

journal homepage: www.elsevier.com/locate/measurement

Non-contact measurement technique for dimensional metrology using optical comb



Wiroj Sudatham^{a,*}, Hirokazu Matsumoto^a, Satoru Takahashi^b, Kiyoshi Takamasu^a

^a Department of Precision Engineering, The University of Tokyo, Hongo 7-3-1 Bunkyo, Tokyo 113-8656, Japan

^b Research Center for Advanced Science and Technology, The University of Tokyo, Komaba 4-6-1, Meguro, Tokyo 153-8904, Japan

ARTICLE INFO

Article history:

Received 6 February 2015

Received in revised form 16 July 2015

Accepted 22 July 2015

Available online 8 August 2015

Keywords:

Non-contact measurement

Pulse interferometer

Absolute length measurement

Dimensional metrology

ABSTRACT

This paper proposes a non-contact pulsed interferometer for dimensional metrology using the repetition frequency of an optical frequency comb. A compact absolute-length measuring system is established for practical non-contact measurement based on a single-mode fiber interferometer. The stability and accuracy of the measurements are compared with those from a commercial incremental laser interferometer. The drifts of both systems have the same tendency and a maximum difference is approximately 0.1 μm . Subsequently, preliminary absolute-length measurements up to 1.5 m were measured. The signal-to-noise ratios of the small signals are improved by a frequency-selective amplifier. It is apparent that the noise is rejected, and the intensity of the interference fringes is amplified, achieving a maximum standard deviation of measurement approximately 1 μm . The proposed technique can provide sufficient accuracy for non-contact measurement in applications such as a simple laser-pulse tracking system.

© 2015 Elsevier Ltd. All rights reserved.

1. Introduction

Recently, demand for high-accuracy measurement for dimensional metrology has increased rapidly. To respond to this requirement, many applications using an optical frequency comb were developed for absolute-length measurements because optical frequency combs have very high accuracy and a high stability of their frequencies. However, those applications, the measuring systems and the optical components are different [1–7].

This paper presents an optical comb application for absolute-length measurement using a single-mode fiber pulsed interferometer technique, which an optical comb is used as the laser source. A repetition frequency of 100 MHz of a general optical frequency comb is transferred to 1 GHz by a fiber type Fabry-Pérot etalon. The stability of the pulsed interferometer is considered because it is a

factor that reflects the reliability of the measurement system versus changes in ambient environmental conditions. The experimental results are compared to measurements obtained with a commercial incremental interferometer. The drifts of both interferometer types are considered in a laboratory without control of air temperature and humidity. Subsequently, a metal ball with a rough surface is used as a target of the interferometer to obtain the length under measurement because the rough metal ball mainly reflects the laser beam to the single-mode fiber interferometer. It is easy to align the laser beam, and this setup also provides three-dimensional target positions. The surface roughness of the metal ball targets is analyzed because it directly influences the envelope inference fringes. Additionally, the requirement of a laser-beam alignment is considered. Finally, a preliminary absolute-length measurement up to 1500 mm was measured by an optical-comb pulsed interferometer, in which a rough metal ball is used as the target. A phase-sensitive analyzing method is used to obtain envelope interference fringes, and

* Corresponding author. Tel./fax: +81 3 5841 6472.

E-mail address: wiroj@nanolab.t.u-tokyo.ac.jp (W. Sudatham).

the measurement results are compensated for the group refractive index of air [8,9] owing to changes in environmental conditions. The proposed measuring system can possibly be used to develop a length-measuring tracking system, and can be applied to verify the coordinate measuring machine (CMM) by the multilateration measurement method [10,11].

2. Measurement principle

2.1. Optical frequency comb

Generally, a laser does not have only one wavelength or frequency, but has some natural bandwidth that is related to the gain medium and the optical cavity. In the optical cavity, the light waves will constructively and destructively interfere with themselves, becoming a formation of standing waves. The discrete sets of frequencies of standing waves are called longitudinal modes. These modes are the only frequencies of light that is allowed to oscillate by the resonant cavity and to oscillate independently. The output of a laser has several thousands of modes. Thus, the output intensity will become nearly constant; this is known as a continuous wave, or cw. If all of the modes of a cw laser are fixed in phase relationship, the lasers will periodically interfere with one another. As a result, the laser produces pulse trains of light and it is said to be mode-locked. Mode-locked lasers generate repetitive, ultrashort optical pulse trains by fixing the relative phases of all of the lasing longitudinal modes [12–15]. These pulses are separated in time that is given by Eq. (1).

$$\tau = \frac{2L}{c} \quad (1)$$

where L is the length of the optical cavity and c is the speed of light in vacuum. Therefore, the mode spacing of the laser will be

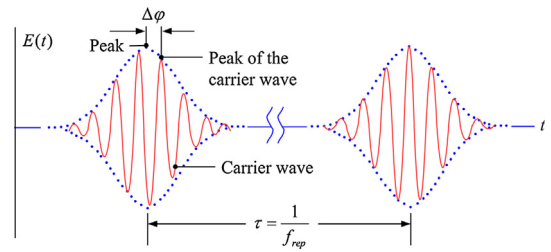
$$\Delta\nu = \frac{1}{\tau} \quad (2)$$

For that reason, the spectrum of each pulse train is separated by the repetition rate of the laser, and the spectral lines are called an optical frequency comb.

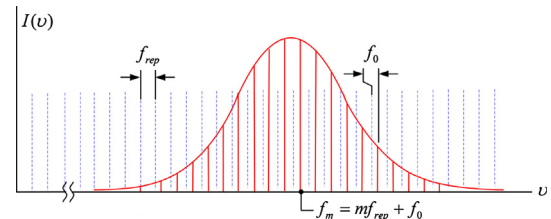
The time and frequency domains of an optical frequency comb are shown in Fig. 1. In the time domain, the pulse train is emitted by a mode-locked laser in the same time as the pulse-to-pulse separation time, $1/f_{rep}$, where f_{rep} is the repetition frequency of the optical frequency comb. In the frequency domain, each shape line is separated equally. The optical frequencies f_m of the comb lines is described as $f_m = mf_{rep} + f_0$, where m is a large integer of order 10^6 and f_0 is the offset frequency resulting from the pulse-to-pulse phase shift ($\Delta\phi$).

2.2. Fabry-Pérot Etalon

A Fabry-Pérot Etalon (etalon) is an interferometer in which the beam of a laser undergoes multiple reflections between two reflecting mirrors [16]. The resulting optical transmission is periodic in wavelength. The transmission of the etalon is at a maximum when the phase difference for a round-trip follows Eq. (3):



(a) Time domain.



(b) Frequency domain.

Fig. 1. (a) Time domain and (b) frequency domain of an optical frequency comb.

$$\frac{2\pi}{\lambda} 2nl \cos \theta = 2m\pi \quad (3)$$

where l is the cavity length of an etalon, θ is the transmission angle, n is the refractive index of the medium and λ is the laser wavelength. Expressing the maximum condition in terms of frequency, the location of transmission peak locations can be written as follows:

$$\nu = m \frac{c}{2nl \cos \theta} \quad (4)$$

Therefore, the frequency separation between successive peaks can be determined. The peak-to-peak frequency separation is called the free spectral range (FSR), and it is given by Eq. (5):

$$\text{FSR} = \Delta\nu = \nu_{m+1} - \nu_m = \frac{c}{2nl \cos \theta} \quad (5)$$

As a result, when an etalon is applied, the repetition frequency of an optical frequency comb is transferred to the high frequency of the FSR. However, the output intensity is reduced when the laser pulse passes through an etalon. Therefore, an optical amplifier is required for some applications.

2.3. Optical comb pulsed interferometer

The diagram of an optical-comb pulsed interferometer is shown in Fig. 2. It is the operating principle of the unbalanced-arm Michelson interferometer. An optical comb generates a pulse train, and the laser pulses are divided into two beams by optical beam splitter (BS). One beam is reflected in the direction of a scanning mirror (M1), while the other is transmitted through a reference position ($OPD = 0$) to a target mirror (M2).

Both reflected light pulses are recombined with the beam that returned from M1 to produce interference fringes when the optical path difference (OPD) of the two arms satisfies the following Eq. (6) [1–3]:

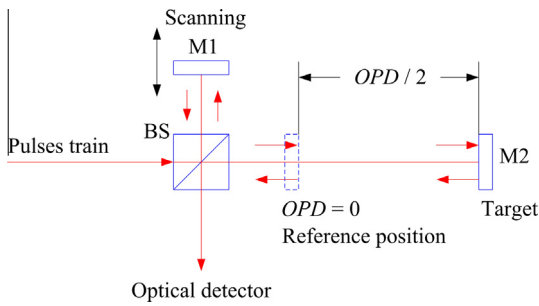


Fig. 2. Principle of an optical-comb pulsed interferometer.

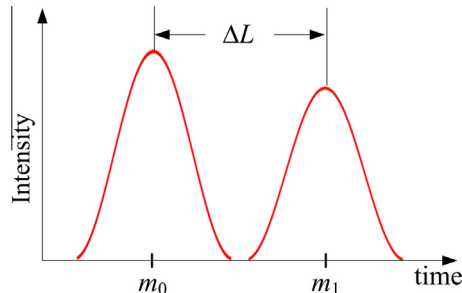


Fig. 3. Envelope interference fringes of the reference position (m_0) and the target (m_1).

$$OPD = \frac{mc}{n_{air}f_{rep}} \quad (6)$$

where m is an integer, n_{air} is the refractive index of air and f_{rep} is the repetition frequency.

Generally, two interference fringes will overlap with each other when observed by an oscilloscope. If the fringes provide a slight displacement (ΔL), the envelope interference fringes will be separated, as shown in Fig. 3. Therefore, the absolute length under measurement is determined as Eq. (7):

$$L = \frac{OPD}{2} + \Delta L \quad (7)$$

In the experiment, two envelope interference fringes are presented in the time domain. Consequently, the relationship between the time scale and length scale must be calibrated to determine the value of ΔL . A linear gauge with a resolution of 10 nm was used to determine this relation. The absolute lengths under measurement also have to compensate for the group refractive index of air owing to the change of environmental conditions by Ciddor's equation [8].

3. Experiments and results

3.1. Stability and accuracy of pulse interferometer

To study measurement stability, a measurement was setup as shown in Fig. 4. An optical-comb pulsed interferometer was paired with an incremental interferometer (Renishaw length-measuring 633 nm, He-Ne laser interferometer).

An optical comb, (C-Fiber femtosecond laser, MenloSystems) was used as the source of laser pulses. The central wavelength is 1560 nm, the output power is 12 mW, and the repetition frequency is 100 MHz, which is stabilized by an Rb-frequency standard. Both measurement systems were prepared in an air-uncontrolled laboratory. Lengths of 150 mm were measured every ten minutes in one hour. The environmental conditions (ambient temperature, relative humidity and air pressure) were also recorded. Then, the drifts of both systems were calculated. The results are illustrated in Fig. 5.

In the experiment, the average value of the ambient temperature, relative humidity, and air pressure were 25.60 °C, 36.5%, and 101.02 kPa; and the maximum variation was approximately 0.2 °C, 1.7% and 10 Pa, respectively. The results in Fig. 5 show that the variations from the average values of both measuring systems have the same drift tendency. The maximum variations of pulse interferometer and incremental interferometer are 0.25 μm and 0.21 μm , respectively. The maximum difference between the two curves is approximately 0.1 μm . Subsequently, the accuracy of the pulse interferometer was considered. According to the incremental interferometer, a comparison requires a long, precise translation stage. The setup diagram for this comparison is shown in Fig. 6(a). Both measuring length systems share the same target to avoid the errors of motion translation, and a photograph of measurement comparison is illustrated in Fig. 6 (b).

In the measurement comparison, a precise translation stage was controlled by a resolution of 0.05 μm , which was moved to a position of approximately 150 mm. Subsequently, the length was measured five times by both measuring systems. The environmental conditions were also recorded, to calculate and compensate for the refractive index of air. The measurement results are listed in Table 1.

3.2. Surface roughness and the fringes of target balls

In this experiment, two rough metal ball with a diameter of approximately 25 mm were used to obtain the envelope interference fringes at the reference position ($OPD = 0$). The measurement setup is illustrated in Fig. 7. One ball is smooth, with R_a of approximately 0.1 μm . The other ball is of rough metal, with R_a of approximately 0.2 μm .

The fringes observation in Fig. 8 indicates that the surface roughness of the target affects the quality of the

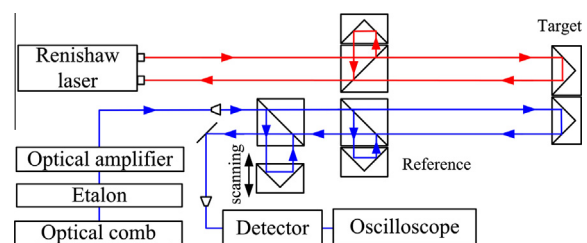


Fig. 4. Measurement setup for study of stability of optical-comb pulsed interferometer compared with an incremental interferometer.

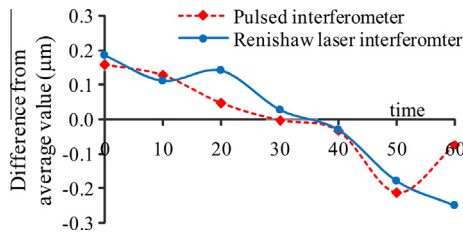


Fig. 5. Measurement stability of pulse interferometer and incremental interferometer.

pattern fringe: a ball with a smooth surface presents a perfect interference fringe, and its intensity is also higher than that of a ball with a rough surface. In addition, if the *Ra* value of the metal ball is higher than 0.2 µm, the interference fringe will disappear because the laser beam cannot reflect to the interferometer system. On the other hand, the intensity of the interference fringe is enhanced if the *Ra* value is better than 0.1 µm. However, aligning the laser beam is not simple if the surface roughness of the metal ball is very smooth ($Ra \ll 0.1 \mu\text{m}$) because the reflected area on the metal ball is too small.

3.3. Preliminary absolute-length measurement up to 1500 mm

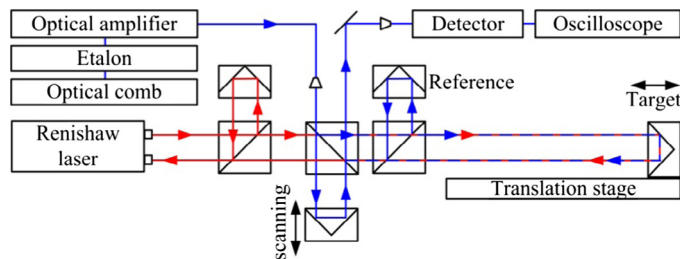
The preliminary measurement setup diagram of the pulsed interferometer with a metal ball target is shown

in Fig. 9. According to the measurement results in Section 3.2, a metal ball with *Ra* approximately 0.1 µm was selected as the target. The ball was moved by 150 mm in each position. Each length was measured 10 times to determine the repeatability of the measurement. In this experiment, although an etalon plays the role of frequency-mode selector, laser power is reduced. In addition, the surface roughness of the target also affects the laser beam that returns to the interferometer. It is very difficult to detect an interference signal by using only a simple optical detector. Consequently, a frequency-selective amplifier was used to amplify a small interference signal. Noise was also rejected by this technique. Fig. 10 shows the results of the measurement.

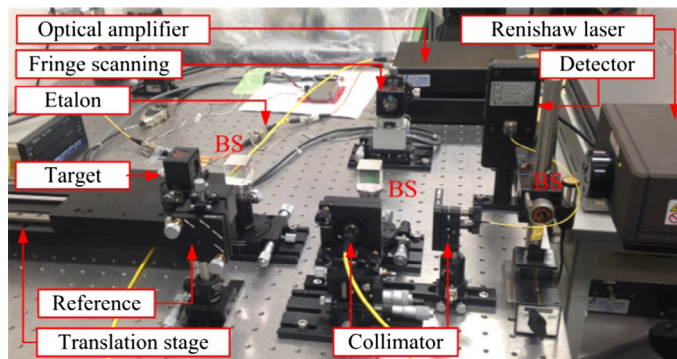
The measurement performance of the proposed technique was evaluated by the repeatability of the measurement of each position. The maximum standard deviation is approximately 1 µm for the absolute length up to 1.5 m. However, the results were measured in an air-uncontrolled laboratory, and the environmental conditions swing between (19.9–22.3) °C, (23.7–28.4) %RH, and (99.7–100.9) kPa for the ambient temperature, air humidity, and air pressure, respectively.

4. Discussion

The stability of an optical-comb pulsed interferometer causes an error in length measurement owing to changes in the refractive index of air. The drift of measurement



(a) Comparison setup of optical-comb pulsed interferometer and incremental laser interferometer



(b) Photograph of measurement comparison.

Fig. 6. (a) Comparison setup diagram, (b) photograph of comparison between optical-comb pulsed interferometer and incremental laser interferometer.

Table 1
Measurement results.

Average of environmental conditions			
	101.02 kPa	25.60 °C	36.5 %RH
No.	Pulsed interferometer (mm)	Incremental interferometer (mm)	Difference (μm)
1	149.85692	149.85689	0.03
2	149.85693	149.85694	-0.01
3	149.85692	149.85682	0.09
4	149.85692	149.85689	0.03
5	149.85693	149.85710	-0.18
SD	0.01	0.10	μm

SD: Measurement standard deviation.

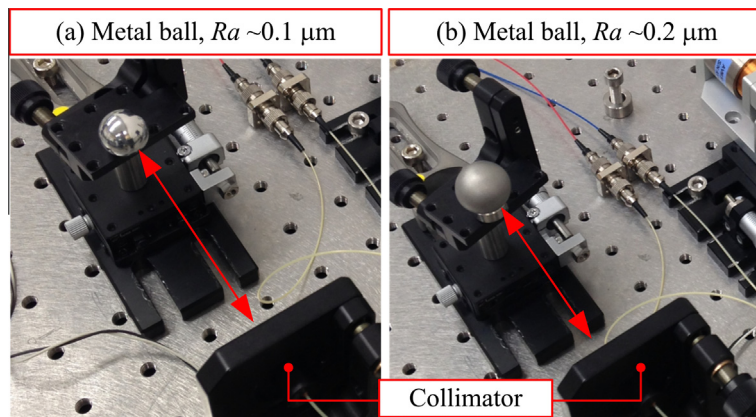


Fig. 7. Optical-comb pulsed interferometer setup with targets at the reference position of measurement: (a) ball is smooth, with R_a of approximately $0.1 \mu\text{m}$, and (b) ball is of rough metal, with R_a of approximately $0.2 \mu\text{m}$.

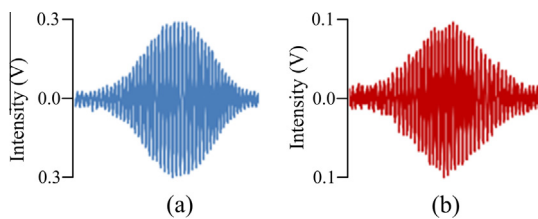


Fig. 8. Interference fringes of (a) a smooth surface, $R_a \sim 0.1 \mu\text{m}$, and (b) a rough surface, $R_a \sim 0.2 \mu\text{m}$ of metal ball targets.

was approximately $0.25 \mu\text{m}$ in one hour. This result shows that the drift was mainly caused by changes in the environmental conditions, while the noise of interference fringe was caused by air fluctuation and mechanical vibration. This is a source of measurement uncertainty, which should be considered in making a precise measurement. In addition, sensors with higher accuracy are required in order to record a change in environment along the entire optical path for compensation.

The roughness of the surface target is significant to the accuracy of measurement. This roughness directly affects fringe acquisition. A suitable surface of a target is one factor that must be considered for applications with a

high-accuracy requirement. Moreover, the roundness and diameter tolerance of the target should also be considered for possible applications. When a metal ball with a diameter of 25 mm is used as the target, a beam misalignment of $\pm 0.2 \text{ mm}$ from the center of the ball will cause an error of measuring length of approximately $1 \mu\text{m}$. However, the error also depends on the surface roughness, roundness, laser beam diameter, and length of measurement. If some area of the ball's surface is not sufficiently smooth, it will affect the error of measurement. In the experiment, using a focusing beam, the repeatability of measurement was improved over using a small spot beam and a large beam diameter. However, the laser beam will be lost when the ball is moved far away from its position. On the other hand, the laser beam is not lost when using a small spot beam and a large beam diameter, but this presents a large standard deviation.

Although an etalon plays the role of frequency mode selector for this application, the power of the laser is reduced. Therefore, the reference mirror type not only achieves a good transmission but also sufficiently reflects the laser beam to produce reference fringes. In the experiment, a sapphire window plate was selected as a reference position ($m=0$) because its transmission property is appropriate for a laser wavelength in the range of

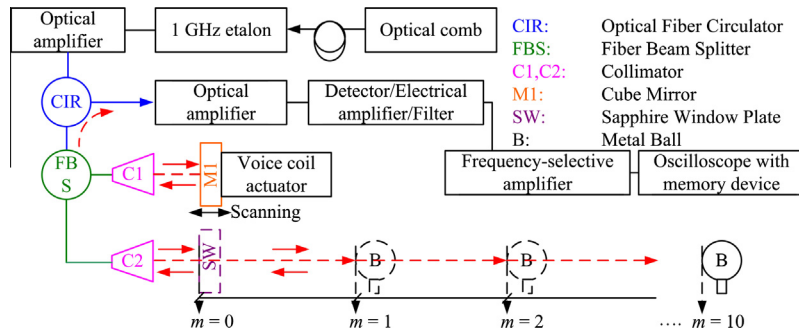


Fig. 9. Measurement set up diagram for absolute length measurement.

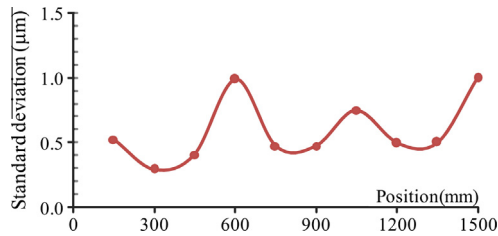


Fig. 10. Measurement results of the absolute length up to 1500 mm.

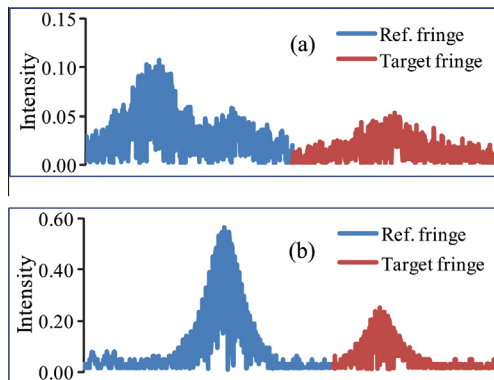


Fig. 11. Interference fringes (a) before and (b) after passing through a frequency-selective amplifier.

1.56 μm . This means the laser power is slightly reduced when the laser passes through a sapphire window plate. Furthermore, an optical amplifier was used to gain the laser power. The interference-fringe signals were amplified by a frequency-selective amplifier. In this case, the phase-sensitive detection method was sufficiently powerful to gain a small signal and reduce noise. Although the power of the laser beam was reduced by an etalon, and the interference fringes were also influenced by the roughness surface of the target, the signal-to-noise ratio of the small signals was improved by a frequency-selective amplifier. It is apparent that the noise is rejected and the interference fringes intensity is amplified, as shown in Fig. 11. Consequently, the interference fringes are captured, and the length observations are also measured.

5. Conclusion

Experiments on absolute-length measurement for dimensional applications have been conducted using an optical-comb pulsed interferometer. The 1-GHz FSR Fabry-Pérot fiber etalon plays the role of a frequency mode selector, and a metal ball is employed as the target of the single-mode fiber interferometer. The measurement accuracy mainly involves the quality of the envelope interference fringes, which correspond to the surface roughness of the target. The drift is mainly sourced from changes in environmental conditions, while the noise of the interference fringe is caused by air fluctuation and mechanical vibration. The stability and accuracy of the measurements are compared with those of a commercial incremental laser interferometer, and the drifts of both systems have the same tendency. The maximum standard deviation is approximately 1 μm for the absolute length measurement up to 1.5 m. The proposed technique can provide sufficient accuracy for non-contact measurement in applications such as a simple laser-pulse tracking system.

References

- [1] X. Wang, S. Takahashi, K. Takamasu, H. Matsumoto, Spatial positioning measurements up to 150 m using temporal coherence of optical frequency comb, *Prec. Eng.* 37 (2013) 635–639.
- [2] C. Narin, S. Takahashi, K. Takamasu, H. Mastsumoto, Step gauge measurement using high-frequency repetition of a mode-locked fiber, in: XX IMEKO World Congress, IMEKO2012, Busan, Korea, TC 14-O-19, 2012, pp. 1–5.
- [3] H. Matsumoto, X. Wang, K. Takamasu, T. Aoto, Absolute measurement of baselines up to 403 m using heterodyne temporal coherence interferometer with optical frequency comb, *Appl. Phys. Exp.* 5 (2012) 046601.
- [4] P. Balling, P. Křen, P. Mašika, S.A. van den Berg, Femtosecond frequency comb based distance measurement in air, *Opt. Exp.* 17 (2009) 9300–9313.
- [5] S. Hyun, Y.-J. Kim, J. Jin, S.-W. Kim, Absolute length measurement with the frequency comb of a femtosecond laser, *Meas. Sci. Technol.* 20 (2009).
- [6] K. Joo, Y. Kim, S.W. Kim, Distance measurements by combined method based on a femtosecond pulse laser, *Opt. Exp.* 16 (2008) 19799–19806.
- [7] J. Ye, Absolute measurement of a long, arbitrary distance to less than an optical fringe, *Opt. Lett.* 29 (2004) 1153–1155.
- [8] P.E. Ciddor, R.J. Hill, Refractive index of air. 2. Group index, *Appl. Opt.* 38 (1999) 1663–1667.
- [9] Y. Yamaoka, K. Minoshima, H. Matsumoto, Direct Measurement of the group refractive index of air with interferometer between adjacent femtosecond pulse, *Appl. Opt.* 41 (2002) 4318–4324.
- [10] J.J. Aguilar, S. Aguado, J. Santolaria, D. Samper, Multilateration in volumetric verification of machine tool, in: XX IMEKO World Congress, Busan, Republic of Korea, September 9–14, 2012.

- [11] W. Klaus, F. Matthias, H. Frank, Measuring large 3D structure using four portable tracking laser interferometer, *J. Meas.* 45 (2012) 2339–2345.
- [12] S.T. Cundiff, J. Ye, Femtosecond optical frequency comb, *Rev. Mod. Phys.* 75 (2003) 325–342.
- [13] D.J. Jones, S.A. Diddams, et al., Carrier-envelope phase control of femtosecond mode-locked laser and direct optical frequency synthesis, *J. Sci.* 288 (2000) 635–639.
- [14] R. Holzwarth, T. Udem, T.W. Hansch, J. Knight, W. Wadsworth, P.S.J. Russell, Optical frequency synthesizer for precision spectroscopy, *Phys. Rev. Lett.* 85 (2000) 2264–2267.
- [15] T. Udem, R. Holzwarth, T.W. Hansch, Optical frequency metrology, *Nature* 416 (2002) 233–237.
- [16] J.M. Vaughan, *The Fabry-Perot Interferometer History, Theory, Practice and Applications*, Taylor & Francis Group, New York, 1989.